Discovery of biased orientations of regulatory motifs affecting transcription of human genes and including known insulators

Naoki Osato[1*]

[1]Department of Bioinformatic Engineering, Graduate School of Information Science and Technology, Osaka University, Osaka 565-0871, Japan

[*]Corresponding author

E-mail address: naokiosato11@gmail.com, nosato@ist.osaka-u.ac.jp

Abstract

Chromatin interactions play essential roles in enhancer-promoter interactions (EPIs) and regulating the transcription of genes. CTCF and cohesin proteins are located at the anchors of chromatin interactions, forming their loop structures. Other DNA binding proteins such as YY1, ZNF143 and SMARCA4 are also reported to be involved in chromatin interactions. However, the overall picture of proteins associated with chromatin interactions and insulator function is still unclear. Here I describe a systematic and comprehensive approach to discover DNA binding motif sequences of transcription factors (TFs), affecting the interaction between enhancers and promoters of genes and their expression by the insulator function of the TFs. This analysis identified 96 biased orientations of DNA motifs of TFs that affected the expression level of putative transcriptional target genes significantly in monocytes, T cells, HMEC and NPC in common, and included known TFs involved in chromatin interaction and insulator function such as CTCF, cohesin (RAD21 and SMC3), YY1 and ZNF143. The 96 biased orientations of DNA motifs contain 64 forward-reverse (FR) and 52 reverse-forward (RF) orientations of DNA motifs (Some TFs have more than one DNA motifs in databases, so the total number is smaller than the sum of FR and RF). To confirm the predicted DNA motifs, first, I compared with chromatin interaction data. Despite the limitation of resolution of chromatin interaction data, for 44 (69%) FR and 28 (54%) RF orientations of DNA motif sequences in $CD4^+$ T cells, EPIs predicted based on an enhancer-promoter association (EPA) that was shortened at the biased orientations of DNA motif sites, overlapped with chromatin interactions significantly

more than other types of EPAs. Second, using gene expression data among 53 tissues, 43 (72%) FR and 40 (80%) RF orientations of DNA motifs showed significantly reduced correlation in expression level of nearby genes separated by the motif sites. Some DNA motif sites of biased orientations of DNA motifs of TFs were found between nearby genes not including DNA motif sites of the known TFs involved in chromatin interactions and between low correlation of expression level of nearby genes. These analyses suggest that the DNA motifs are associated with insulator functions.

Keywords: transcriptional target genes, gene expression, transcription factors, enhancer, enhancer-promoter interactions, chromatin interactions, CTCF, cohesin, open chromatin regions, co-location of transcription factors, homodimer, heterodimer, complex

Background

Chromatin interactions play essential roles in enhancer-promoter interactions (EPIs) and regulating the transcription of genes. CTCF and cohesin proteins are located at the anchors of chromatin interactions, forming their loop structures. CTCF has insulator function limiting the activity of enhancers into the loops (Fig. 1A). The DNA binding sequence of CTCF indicate its orientation bias at chromatin interaction anchors – forward-reverse (FR) orientation is frequently observed (Rao et al. 2014; de Wit et al. 2015; Guo et al. 2015). Other DNA binding proteins such as ZNF143, YY1 and SMARCA4 (BRG1) are involved in chromatin interaction and EPI (Bailey et al. 2015; Barutcu et al. 2016; Weintraub et al. 2017). ZNF143 is known to bind more to promoter

55 of genes than distal regions, establishing looping with distal element bound by CTCF
56 (Bailey et al. 2015). DNA binding motif sequence of ZNF143 is significantly enriched
57 at both chromatin interaction anchors (Z-score > 7), whereas DNA binding motif
58 sequence of YY1 does not seem to be enriched (Z-score < 2; Bailey et al. 2015 Figure
59 2a). CTCF, cohesin, ZNF143, YY1 and SMARCA4 have various biological functions
60 other than chromatin interaction. These transcription factors (TFs) are bound in open
61 chromatin regions near transcriptional start sites (TSS) as well as chromatin interaction
62 anchors, which may reduce the enrichment of the DNA motif sites of the TFs at
63 chromatin interaction anchors.

64 Computational approaches to predict chromatin interactions were developed
65 (Schreiber et al. 2017; Zhang et al. 2017). However, they were not intended to find
66 DNA motif sequences of TFs involved in chromatin interactions. (Xie et al. 2005)
67 mentioned in Conclusion section that the next challenge will be to develop systematic
68 methods to discern the specific functions of these motifs in a genome-wide fashion.

69 DNA binding proteins involved in chromatin interactions are considered to affect
70 the transcription of genes in the loops formed by chromatin interactions. To confirm this
71 notion, I previously found that the expression level of human putative transcriptional
72 target genes of a TF was significantly changed, according to the criteria of
73 enhancer-promoter association (EPA) (Osato 2018). An EPA was shortened at the FR
74 orientation of CTCF binding sites, and transcriptional target genes of each TF bound in
75 enhancers and promoters were predicted based on the EPA (Fig. 1B). The expression
76 levels of the transcriptional target genes were significantly different, compared with the

77 expression levels of transcriptional target genes of TFs predicted based on only
78 promoters (or closed chromatin regions). The expression levels tend to be increased in
79 monocytes and $CD4^+$ T cells, implying that enhancers activate the transcription of genes.
80 The expression levels tend to be decreased in ES and iPS cells, implying that enhancers
81 repress the transcription of genes. The expression level of putative transcriptional target
82 genes of a TF bound in enhancers is changed significantly, when EPIs are predicted
83 properly using the insulator sites of CTCF in cell types. This suggests that the difference
84 of the expression level would reflect the accuracy of prediction of transcriptional target
85 genes of a TF based on a given EPA. Using this approach, I planned to search for other
86 DNA binding proteins involved in chromatin interactions, affecting the expression level
87 of putative transcriptional target genes through their insulator function.

88 Experimental analyses of chromatin interactions in molecular biology have
89 technical limitations: chromatin interaction data are altered, according to experimental
90 techniques, the number of reads of DNA sequencing and even replication sets of the
91 same cell type. Chromatin interaction data may not be saturated enough to contain all
92 chromatin interactions and may include experimental noises such as ligation error.
93 Avoiding the technical limitations of experimental analyses, here I searched
94 computationally for DNA motif sequences of TFs, affecting EPI and the expression
95 level of putative transcriptional target genes in monocytes, T cells, HMEC and NPC
96 without using chromatin interaction data. Then, putative EPIs and DNA motif sites of
97 TFs were compared with chromatin interaction and gene expression data.
98

99 ## Results

100 **Search for biased orientations of DNA motif sequences**

101 Transcription factor binding sites (TFBSs) were predicted using open chromatin
102 regions and DNA motif sequences of transcription factors (TF) collected from various
103 databases and journal papers (see Methods). Transcriptional target genes were predicted
104 based on TFBS in promoters and enhancers. An enhancer-promoter association (EPA)
105 was shortened at the DNA binding motif sites of a TF acting as insulator such as CTCF
106 and cohesin (RAD21 and SMC3) (Fig. 1B). To find DNA motif sequences of TFs with
107 insulator function, other than CTCF and cohesin, affecting the expression level of genes,
108 An EPA was shortened at the DNA motif sites of a putative insulator TF, and
109 transcriptional target genes of each general TF bound in (i) distal open chromatin
110 regions (enhancers) and (ii) closed chromatin regions in promoters were predicted based
111 on the EPA, in order to estimate the enhancer activity of each general TF. The ratio of
112 expression level of putative transcriptional target genes of each TF between (i) and (ii)
113 was calculated. The distribution of the ratios of all general TFs was compared among
114 forward-reverse (FR), reverse-forward (RF) orientations and non-orientation (i.e.
115 without considering orientation) of DNA motif sites of an insulator TF shortening an
116 EPA using Mann-Whitney test, two-sided (p-value $< 10^{-7}$), and putative insulator TFs
117 with significant differences of the distributions of the ratios of expression level among
118 FR, RF orientations and non-orientation were enumerated (Fig. 2A).

119 To confirm the prediction of TFBS, the distributions of TFBS were examined in
120 the human genome. TFBS involved in chromatin interactions were identified near TSS

121 (Fig. 2B). ZNF143 is known to bind to promoter of genes establishing looping with
122 distal element bound by CTCF (Fig. 5) (Bailey et al. 2015). YY1 is multi-functional
123 transcriptional regulator and is involved in transcriptional activation, repression and
124 initiation (Shrivastava and Calame 1994; Xi et al. 2007). Most of DNA motif sites of
125 the TFs were identified in intergenic and intron regions of the human genome (Fig. 2C).

126 Several hundreds of FR and RF orientations of DNA motifs of TFs were found in
127 monocytes, T cells, human mammary epithelial cells (HMEC) and neural progenitor
128 cells (NPC) (Fig. 3). The number of the TFs seemed to be changed, according to the
129 number of DNase-seq reads, since the number of the reads in monocyte is larger than
130 the other three cell types. When DNase-seq reads increase, more TFBS may be
131 predicted to some extent. Total 96 of biased (64 FR and 52 RF) orientations of DNA
132 binding motif sequences of TFs were discovered in the four cell types in common,
133 whereas non-orientation of DNA binding motif sequences of TFs were not detected (Fig.
134 3; Table 1; Supplemental material). The FR orientation of DNA motif sequences
135 included CTCF, cohesin (RAD21 and SMC3), YY1 and ZNF143, which are involved in
136 chromatin interaction and EPI.

137 Without considering the difference of orientations of DNA binding motif
138 sequences among cell types, 175 biased orientations of DNA binding motif sequences
139 of TFs were found in the four cell types in common. These numbers (96 and 175) are
140 unique numbers of TFs with biased orientations of DNA motifs, and not the unique
141 numbers of DNA motifs. Possible causes of the number 175 increased from 96 are as
142 follows: (1) a TF or an isoform of the same TF may bind to a different DNA binding

143 motif sequence, according to cell types and/or in the same cell type. About 50% or more
144 of alternative splicing isoforms are differently expressed among tissues, indicating that
145 most alternative splicing is subject to tissue-specific regulation (Das et al. 2007; Wang
146 et al. 2008; Chen and Manley 2009). (2) The same TF has several DNA binding motif
147 sequences, and in some cases one of the motif sequences is almost the same as the
148 reverse complement sequence of another motif sequence of the same TF in the same or
149 different databases of TFs. (3) I previously found that a complex of TFs would bind to a
150 slightly different DNA binding motif sequence from the combination of DNA binding
151 motif sequences of TFs composing the complex in *C. elegans* (Tabuchi et al. 2011). In
152 other reports, the difference of binding specificity of pairs of TFs was investigated
153 (Jolma et al. 2015). Cofactors also contribute to alter binding specificity of TFs (Ansari
154 and Peterson-Kaufman 2011; Slattery et al. 2011; Merabet and Mann 2016). These
155 increase the variety and number of (biased orientations of) DNA binding motif
156 sequences of a TF, which are potentially involved in different biological functions
157 among cell types.
158
159 **Comparison with chromatin interaction data**
160 To ask whether the biased orientations of DNA motif sequences are associated
161 with chromatin interaction, enhancer-promoter interactions (EPIs) predicted based on an
162 enhancer-promoter association (EPA) were compared with chromatin interaction data.
163 EPIs predicted based on an EPA were compared with three replications (B2T1, B2T2
164 and B3T1) of HiChIP chromatin interaction data in $CD4^+$ T cells separately (Mumbach

165 et al. 2017). The resolutions of HiChIP chromatin interaction data and EPIs were
166 adjusted to 5 kilobases (kb). The number of unique HiChIP cis (i.e. in the same
167 chromatin) chromatin interactions was 19,926,360 at 5 kb resolution in B2T1
168 replication of T cells, 666,149 at 5 kb resolution with ≥1,000 counts for each
169 interaction and 78,209 at 5 kb resolution with ≥6,000 counts for each interaction
170 (Supplemental material). EPI were predicted based on three types of EPAs: (i) EPA
171 shortened at the FR or RF orientation of DNA motif sites of a TF with putative insulator
172 function such as CTCF, (ii) EPA shortened at the DNA motif sites of a TF without
173 considering their orientation, and (iii) EPA without being shortened by DNA motif sites.
174 For total 201 biased orientations [133 (49%) FR and 90 (43%) RF of 273 FR and 211
175 RF] of DNA motif sequences in T cells, which included CTCF, cohesin (RAD21 and
176 SMC3), ZNF143 and YY1 in three replications (B2T1, B2T2, and B3T1), a
177 significantly higher ratio of EPIs overlapped with HiChIP chromatin interactions with
178 ≥1,000 counts for each interaction in EPA (i) than the other types of EPA (ii) and (iii) in
179 T cells (Table 2). When comparing EPIs predicted based on only EPA (i) and (iii) with
180 the chromatin interactions, for total 390 biased orientations [261 (96%) FR and 199
181 (94%) RF of 273 FR and 211 RF] of DNA motif sequences in T cells, a significantly
182 higher ratio of EPIs overlapped with the chromatin interactions in EPA (i) than EPA (iii)
183 (Table 2; Supplemental material). The difference between EPIs predicted based on EPA
184 (i) and (ii) seemed to be difficult to distinguish using the chromatin interaction data and
185 a statistical test in some cases. However, as for the difference between EPIs predicted
186 based on EPA (i) and (iii), a larger number of biased orientations of DNA motif

187 sequences were correlated with chromatin interaction data. Most of biased orientations
188 of DNA motif sequences (95%) were correlated with chromatin interactions, when
189 comparing EPIs predicted based on EPA (i) and (iii) with HiChIP chromatin interactions.
190 Chromatin interaction data were obtained from different samples from DNase-seq open
191 chromatin regions, so individual differences may exist. Individual differences of
192 chromatin interactions were larger than those of open chromatin regions (Mumbach et
193 al. 2017).

194 Additionally, to confirm these tendencies of comparison of EPIs with HiChIP
195 chromatin interactions, the same analysis was conducted using HiChIP chromatin
196 interaction data in Th17, Treg and GM12878 cells. For total 128 biased orientations [76
197 (38%) FR and 64 (35%) RF of 200 FR and 183 RF] of DNA motif sequences in Th17
198 cells, which included CTCF, cohesin (RAD21 and SMC3), ZNF143 and YY1 in three
199 replications (B1T2, B2T1, and B3T1), a significantly higher ratio of EPIs overlapped
200 with HiChIP chromatin interactions in EPA (i) than the other types of EPA (ii) and (iii)
201 (Supplemental material). When comparing EPIs predicted based on only EPA (i) and
202 (iii) with the chromatin interactions, for total 282 biased orientations [182 (91%) FR
203 and 162 (89%) RF of 200 FR and 183 RF] of DNA motif sequences, a significantly
204 higher ratio of EPIs overlapped with the chromatin interactions in EPA (i) than EPA (iii)
205 (Supplemental material).

206 In Treg cells, chromatin interactions in one biological replication were overlapped
207 with EPIs, but those in the other two biological replications were less overlapped with
208 EPIs, so the one replication (B3T1) was used for this analysis. For total 281 biased

209 orientations [154 (53%) FR and 176 (54%) RF of 290 FR and 323 RF] of DNA motif
210 sequences, which included CTCF, cohesin (RAD21 and SMC3), ZNF143 and YY1, a
211 significantly higher ratio of EPIs overlapped with HiChIP chromatin interactions in EPA
212 (i) than the other types of EPA (ii) and (iii) (Supplemental material). When comparing
213 EPIs predicted based on only EPA (i) and (iii) with the chromatin interactions, for total
214 482 biased orientations [283 (98%) FR and 309 (96%) RF of 290 FR and 323 RF] of
215 DNA motif sequences, a significantly higher ratio of EPIs overlapped with the
216 chromatin interactions in EPA (i) than EPA (iii) (Supplemental material).

217 In GM12878 cells, for total 168 biased orientations [96 (38%) FR and 98 (35%)
218 RF of 229 FR and 237 RF] of DNA motif sequences, which included CTCF, cohesin
219 (RAD21 and SMC3), ZNF143 and YY1 in two replications (B1 and B2), a significantly
220 higher ratio of EPIs overlapped with HiChIP chromatin interactions in EPA (i) than the
221 other types of EPA (ii) and (iii) (Supplemental material). When comparing EPIs
222 predicted based on only EPA (i) and (iii) with the chromatin interactions, for total 366
223 biased orientations [218 (95%) FR and 227 (96%) RF of 229 FR and 237 RF] of DNA
224 motif sequences, a significantly higher ratio of EPIs overlapped with the chromatin
225 interactions in EPA (i) than EPA (iii) (Supplemental material).

226 In situ Hi-C data in HMEC, which are available in 4D nucleome data portal, were
227 compared with putative EPIs. The number of unique in situ Hi-C cis chromatin
228 interactions was 121,873,642 at 3 kb resolution. For total 222 biased orientations [155
229 (50%) FR and 108 (40%) RF of 310 FR and 269 RF] of DNA motif sequences, which
230 included CTCF, cohesin (RAD21 and SMC3), ZNF143 and YY1, a significantly higher

231 ratio of EPIs overlapped with in situ Hi-C chromatin interactions (≥1 count for each
232 interaction, i.e. all interactions) in EPA (i) than the other types of EPA (ii) and (iii)
233 (Supplemental material). When comparing EPIs predicted based on only EPA (i) and
234 (iii) with the chromatin interactions, for total 406 biased orientations [268 (86%) FR
235 and 230 (86%) RF of 310 FR and 269 RF] of DNA motif sequences, a significantly
236 higher ratio of EPIs overlapped with the chromatin interactions in EPA (i) than EPA (iii)
237 (Supplemental material). There were six replications of in situ Hi-C experimental data
238 of HMEC, but other replications contained much smaller number of chromatin
239 interactions. The HiChIP chromatin interaction data in T cells were expected to be
240 enriched with enhancer-promoter interactions, since they were produced with H3K27ac
241 antibody to capture chromatin interactions. In situ Hi-C data consist of all types of
242 chromatin interactions and thus, contain a smaller number of enhancer-promoter
243 interactions than HiChIP data. Chromatin interactions with a small number of counts
244 may be artifacts occurred by ligation errors during experiments (Lieberman-Aiden et al.
245 2009; Yardimci et al. 2019). Therefore, other replications of in situ Hi-C data with a
246 smaller number of chromatin interactions will not be available for this analysis.

247 Promoter capture Hi-C data of NPC was downloaded and analyzed in the same
248 procudure as T cell and HMEC (Jung et al. 2019). The number of unique promoter
249 capture Hi-C cis chromatin interactions was 9,436,689 at 5 kb resolution. For total 109
250 biased orientations [61 (28%) FR and 60 (25%) RF of 205 FR and 241 RF] of DNA
251 motif sequences, which included CTCF, cohesin (RAD21 and SMC3), ZNF143 and
252 YY1, a significantly higher ratio of EPIs overlapped with promoter capture Hi-C

253 chromatin interactions (≥1 count for each interaction, i.e. all interactions) in EPA (i)
254 than the other types of EPA (ii) and (iii) (Supplemental material). When comparing EPIs
255 predicted based on only EPA (i) and (iii) with the chromatin interactions, for total 186
256 biased orientations [99 (48%) FR and 103 (43%) RF of 205 FR and 241 RF] of DNA
257 motif sequences, a significantly higher ratio of EPIs overlapped with the chromatin
258 interactions in EPA (i) than EPA (iii) (Supplemental material).

259 All three types of chromatin interaction data (HiChIP, in situ Hi-C and promoter
260 capture Hi-C) indicated that EPIs predicted based on EPA (i) that was shortened at DNA
261 motif sites of known TFs involved in chromatin interactions (CTCF, RAD21, SMC3,
262 ZNF143 and YY1), overlapped with more chromatin interactions than the other EPA (ii)
263 and (iii) in six cell types (T cells, Th17, Treg, GM12878, HMEC and NPC). In
264 monocyte, Hi-C data was available, but it was not analyzed, due to the low resolution of
265 chromatin interaction data (50 kb).

266 The biased orientations of DNA motif sites of known TFs involved in chromatin
267 interactions such as CTCF, RAD21, SMC3, YY1 and ZNF143 may be overlapped with
268 the biased orientations of DNA motif sites of other TFs, and thus, they showed a
269 significantly higher ratio of EPIs overlapped with chromatin interactions in EPA (i) than
270 the other types of EPA (ii) and (iii). However, among 273 FR and 211 RF orientations of
271 DNA motifs of TFs not including the known TFs in T cells, the DNA motif sites of only
272 15 (6%) FR and 9 (4%) RF orientations of DNA motifs of TFs overlapped with ≥ 60%
273 of DNA motif sites of biased orientations of DNA motifs of either of the known TFs at 5
274 kb resolution.

275 Moreover, to investigate the enhancer activity of EPIs, the distribution of
276 expression level of putative target genes of EPIs was compared between EPIs
277 overlapped with HiChIP chromatin interactions and EPIs not overlapped with them.
278 Though the target genes of EPIs were selected from top 4,000 transcripts (genes) in
279 terms of the expression level of all transcripts (genes) excluding transcripts not
280 expressed in T, Th17, Treg and GM12878 cells separately, target genes of EPIs
281 overlapped with chromatin interactions indicated a significantly higher expression level
282 than EPIs not overlapped with them, suggesting that EPIs overlapped with chromatin
283 interactions activated the expression of target genes in the four cell types. For almost all
284 (99% - 100%) FR and RF orientations of DNA motifs, a significantly higher expression
285 level of putative target genes of EPIs overlapped with chromatin interactions than EPIs
286 not overlapped in the four cell types. When a biased orientation of DNA motif showed a
287 significantly higher expression level of putative target genes of EPIs overlapped with
288 chromatin interactions than EPIs not overlapped, '1' was marked with in the tables of
289 comparison between EPIs and HiChIP chromatin interactions in Supplemental material.
290 DNA motifs showing a significantly lower expression level or not showing a significant
291 difference of expression level were not observed in this analysis. HiChIP data were
292 produced using H3K27ac antibody, so chromatin interactions acting as repressor would
293 not be identified. However, for in situ Hi-C and promoter capture Hi-C data in HMEC
294 and NPC, the significant difference of expression level of putative target genes of EPIs
295 was observed in a small percentage (less than 1%) of biased orientations of DNA
296 motifs.

297

298 **Correlation of expression level of gene pairs separated by DNA motif sites of a TF**

299 To ask whether the biased orientations of DNA motif sites affect gene expression,
300 I compared the expression level in monocytes of protein-coding genes the most closely
301 located to upstream and downstream of biased orientations of DNA motif sites in the
302 human genome. The expression levels of closely located genes including divergent gene
303 pairs tend to be correlated among tissues (Purmann et al. 2007; Xie et al. 2007). When a
304 biased orientation of DNA motif sites serve as insulator (e.g. CTCF), the correlation of
305 gene expression level would be reduced. Among 96 biased (64 FR and 52 RF)
306 orientations of DNA motifs of TFs found in common in monocytes, T cells, HMEC and
307 NPC, TFs with $\geq$50 genomic locations of the DNA motif sites were selected, after the
308 elimination of ubiquitously expressed genes among 53 tissues and DNA motif sites near
309 the genes with coefficient of variance (CV) <90. After this filtering, 43 (72%) FR and
310 40 (80%) RF of 60 FR and 50 RF showed significantly lower correlations of expression
311 levels of gene pairs separated by the DNA motif sites of a TF than the correlations of all
312 pairs of neighbor genes with intergene distance <1 megabase (Mb) (Mann-Whitney test,
313 p-value < 0.05) (Table 3). The FR and RF orientations of TFs included known TFs
314 involved in chromatin interactions such as CTCF, RAD21, SMC3, YY1 and ZNF143.
315 Top 20 of the FR and RF orientations of DNA motifs were selected in ascending order
316 of the median correlation coefficient of expression levels of gene pairs separated by the
317 DNA motif sites of a TF. The 20 TFs included known TFs involved in chromatin
318 interactions such as CTCF, RAD21 and SMC3 (Fig. 4) (Mann-Whitney test, p-value <

319 0.01). Instead of using all DNA motif sites of a TF, when DNA motif sites of a TF were
320 limited to sites examined for biased orientations of DNA motifs in an EPA, 33 (60%)
321 FR and 36 (77%) RF of 55 FR and 47 RF showed significantly lower correlations of
322 expression levels of gene pairs separated by the DNA motif sites (Supplemental
323 material). With intergene distance <20 kb, 21 (34%) FR and 8 (15%) RF of 62 FR and
324 52 RF showed significantly lower correlations of expression levels of gene pairs
325 separated by the DNA motif sites of a TF than the correlations of all pairs of neighbor
326 genes (Supplemental material).

327 A large number of DNA motif sites of a TF tend to show significantly lower
328 correlations of gene expression (Median numbers of DNA motif sites showing
329 significantly lower correlations were 656 and 479 for FR and RF respectively, and
330 median numbers of DNA motif sites not showing lower correlations significantly were
331 122 and 115 for FR and RF respectively. Mann-Whitney test p-value = 0 and < 10^{-10} for
332 FR and RF respectively). This suggests that if the criteria to examine the correlations of
333 expression levels of gene pairs separated by DNA motif sites are more stringent, and
334 thus the number of DNA motif sites is reduced, it would be more difficult to identify
335 using a statistical test the difference of correlations of expression levels of gene pairs
336 separated by the reduced DNA motif sites of TFs, particularly for TFs with a small
337 number of DNA motif sites.

338 Among 91 biased orientations of DNA motifs of TFs found in common in the
339 four cell types, after removing five known TFs involved in chromatin interactions such
340 as CTCF, RAD21, SMC3, YY1 and ZNF143, DNA motif sites of 88 TFs were located

341 at ≥1 genomic regions between gene pairs not including DNA motif sites of the known
342 TFs, and at ≥1 genomic regions between low correlation (< 0.13) of expression level of
343 gene pairs (when ubiquitously expressed genes among 53 tissues were eliminated with
344 CV <90. The median correlation coefficient of expression level of all pairs of nearby
345 genes is 0.17, Table 3). DNA motif sites of 52 TFs were placed at ≥10 genomic
346 regions.
347
348 **Co-location of biased orientations of DNA motif sites of TFs**
349 To examine the association of biased orientations of DNA binding motif
350 sequences of TFs, co-location of the DNA binding motif sequences within 200bp to
351 each other, which is close to the length of core DNA around octamer of core histone
352 (146bp), that is, the length of the minimum open chromatin region, was analyzed in
353 monocytes, T cells, HMEC and NPC. The same pairs of DNA binding motif sequences
354 in upstream and downstream of genes in EPAs were enumerated, and the pairs of DNA
355 binding motif sequences found in ≥100 genomic regions were listed (Table 4;
356 Supplemental material). Majority of pairs of DNA motif sites overlapped with more
357 than 1 base, but the same tendency was found in the analysis of DNA motif sites of all
358 TFs (Supplemental material). CTCF was partially overlapped with cohesin RAD21 and
359 SMC3 (Table 4). Top 30 pairs of FR and RF orientations of DNA motifs overlapped or
360 co-localized were shown (Table 4). Total numbers of unique pairs of DNA motif sites of
361 TFs overlapped or co-localized were 404 (FR) and 662 (RF) in monocytes, consisting of
362 177 (39% of all FR) and 218 (43% of all RF) unique DNA motifs. Only ten overlapping

363 or co-location of DNA motifs of TFs were identified in the four cell types in common,
364 including pairs of CTCF, RAD21, SMC3 and YY1. This implies that most of
365 overlapping and co-location of DNA motifs of TFs serve in cell-type-specific manner
366 (Supplemental material). Pairs of biased orientations of DNA binding motifs of TFs
367 tend to overlap, and relatively a small number of motifs are co-localized in upstream
368 and downstream of genes. Overlapping DNA motifs act as DNA binding sites of several
369 TFs simultaneously or competitively (Ackerman et al. 1991; Yoon and Chikaraishi
370 1992; Ansari and Peterson-Kaufman 2011; Slattery et al. 2011; Chatterjee et al. 2012;
371 He et al. 2015; Kin et al. 2016; Merabet and Mann 2016). CTCF and cohesin function
372 coordinately with another TF and a protein such as Klf4 and Brd2 (Wei et al. 2013; Hsu
373 et al. 2017). Klf4 recruits cohesin to the Oct4 enhancer region. BRD2 supports
374 boundary (insulator) activity of CTCF. The analysis of 457 ChIP-seq data sets on 119
375 human TFs showed that secondary motifs were detected in addition to the canonical
376 motifs of the TFs, indicating tethered binding and co-binding between multiple TFs
377 (Wang et al. 2012a). The authors observed significant position and orientation
378 preferences between many co-binding TFs. Overlapping DNA motif sites of TFs found
379 in this study may not be artifact, but biologically functional. Though repeat sequences in
380 human genome were masked, more than a hundred of pairs of DNA motif sites
381 overlapped at hundreds or thousands upstream and downstream regions of genes.
382

383 **Discussion**

384 The approach in this study is an initial comprehensive method to find DNA motif

385 sequences of transcription factors (TFs) associated with chromatin interaction and
386 insulator function. DNA motif sequences were searched from open chromatin regions of
387 monocytes, T cells, HMEC and NPC. Total 96 biased [64 forward-reverse (FR) and 52
388 reverse-forward (RF)] orientations of DNA motif sequences of TFs were found in the
389 four cell types in common, whereas non-orientation (i.e. without considering
390 orientation) of DNA motif sequences of TFs were not found to affect the expression
391 level of putative transcriptional target genes, suggesting that an enhancer-promoter
392 association (EPA) shortened at the FR or RF orientation of DNA motif sites of a TF
393 includes more accurate prediction of enhancer-promoter interactions (EPIs), which were
394 supported by the comparisons with chromatin interaction and gene expression data.

395 To predict DNA motif sites of TFs, I tried several tools and methods, and then
396 used protein interaction quantitation (PIQ) tool (Sherwood et al. 2014). PIQ predicts
397 DNA motif sites of TFs by reducing noises of DNase-seq data, and the comparison of
398 the prediction with ChIP-seq data has revealed that PIQ shows a better performance
399 than other tools and digital genome footprinting (DNase-DGF). The prediction of DNA
400 motif sites of TFs using PIQ in this study increased the number of biased orientations of
401 DNA motif sequences of TFs, reducing the number of non-orientation of DNA motif
402 sequences of TFs. At first, the number of predicted DNA motif sites of TFs was
403 expected to increase, relative to using consensus DNA sequences of TFs, which seemed
404 to be stringent to find all DNA motif sites of a TF in the genome. However, the number
405 of DNA motif sites was almost the same or slightly decreased, compared with the
406 analysis of consensus DNA sequences, suggesting that PIQ increases true positive

407 predictions of DNA motif sites, reducing false positive predictions.

408 When forming a homodimer or heterodimer with another TF, TFs may bind to
409 genome DNA with a specific orientation of their DNA binding sequences (Fig. 5). The
410 approach in this study would be able to identify TFs forming heterodimer. If the DNA
411 motif site of only the mate to a pair of TFs was found in an EPA, the EPA was shortened
412 at one side of the DNA motif site, and transcriptional target genes were predicted based
413 on the EPA shortened at the side. In this analysis, the mate to both heterodimer and
414 homodimer of TFs can be tested to examine the effect on the expression level of
415 transcriptional target genes predicted based on the EPA shortened at one side. Biased
416 orientations of DNA motif sequences may also be found in forward-forward or
417 reverse-reverse orientation.

418 TFs that are multi-functional transcriptional regulator such as YY1 may not
419 indicate a strong biased orientation of their DNA motif sites. Though some proportion
420 of DNA motif sites of a TF involved in chromatin interaction and insulator function lie
421 in biased orientation in the genome, the other DNA motif sites of the TF may not form a
422 dimer with another TF, and not be present in a specific orientation in the genome. Thus,
423 overall proportion of biased orientations of DNA motif sites of a TF may be reduced, so
424 that a statistical test cannot detect it.

425 The approach in this study was tested to search for repeat sequences serving as
426 insulator sites and affecting the expression level of putative transcriptional target genes
427 of TFs. A small number of repeat sequences were identified and included MIR, which
428 acts as insulators (Wang et al. 2015).

429 CTCF and cohesin-binding sites are frequently mutated in cancer (Katainen et al.
430 2015). Some biased orientations of DNA motif sequences would be involved in
431 chromatin interactions and might be associated with diseases including cancer.

432 The analyses taken here suggest that biased orientations of DNA motifs of
433 discovered insulator TFs affect enhancer-promoter interactions and the expression level
434 of putative transcriptional target genes of general TFs bound in enhancers and
435 promoters through insulator function. This gives insight into the nature of insulators and
436 contributes to the researches of functions and molecular mechanisms of chromatin
437 interactions, TFs, transcriptional regulation and transcriptional cascades.

438

439 Methods

440 Search for biased orientations of DNA motif sequences

441 To identify transcription factor binding sites (TFBSs) from open and closed
442 chromatin regions, TRANSFAC (2019.2), JASPAR (2018), UniPROBE (2018),
443 high-throughput SELEX, transcription factor binding sequences of ENCODE ChIP-seq
444 data, and HOCOMOCO version 9 and 11 were used to predict insulator sites
445 (Wingender et al. 1996; Newburger and Bulyk 2009; Portales-Casamar et al. 2010; Xie
446 et al. 2010; Zhao and Stormo 2011; Jolma et al. 2013; Kheradpour and Kellis 2014;
447 Kulakovskiy et al. 2018). TRANSFAC (2019.2) was used to analyze enhancer-promoter
448 interactions, because these data were sufficient to identify biased orientations of DNA
449 motif sequences of insulator TFs with less computational time, reducing the number of
450 non-orientation of DNA motif sequences of TFs. To reduce false positive prediction of

451 DNA motif sites of TFs in open chromatin regions, DNA motif search was performed
452 by protein interaction quantitation (PIQ) tool with 12,249 position frequency matrices
453 converted from DNA motifs of vertebrate TFs in the above databases and DNase-seq
454 data from GEO and ENCODE database (GSM1024791 $CD14^+$ monocytes; GSM665812
455 $CD4^+$ T cell; GSM736634 Human mammary epithelial cell, HMEC; GSM878615
456 Neural progenitor cell, NPC; ENCFF263GMV, ENCFF886XEV Th17; GSM1024741
457 Treg; GSM736620 GM12878) (Sherwood et al. 2014). To find open chromatin regions
458 associated with enhancer (and promoter) activity, narrow peaks of ChIP-seq
459 experimental data of H3K27ac were predicted using macs2 callpeak (GEO:
460 GSM773004) (Zhang et al. 2008). To predict DNA motif sites of TFs from closed
461 chromatin regions, another method was employed. Position weight matrices of
462 vertebrate transcription factor binding sequences were converted into DNA consensus
463 sequences, which consist of alphabet of 15 characters (the four bases A, C, G, T, the six
464 two-fold degenerate IUPAC codes R=[AG], Y=[CT], K=[GT], M=[AC], S=[GC],
465 W=[AT], the four three-fold degenerate IUPAC codes B=[CGT], D=[AGT], H=[ACT],
466 V=[ACG], and the four-fold degenerate character N=[ATGC]) using convert matrix in
467 RSAT website (van Helden 2003). Transcription factor binding sequences were
468 searched from narrow peaks of DNase-seq data in repeat-masked hg19 genome
469 sequences using Match tool in TRANSFAC with similarity score cutoff of 1 after
470 transforming the DNA consensus sequences of TFs into position frequency matrixes for
471 Match search (Kel et al. 2003). Repeat-masked hg19 genome sequences were
472 downloaded from UCSC genome browser (http://genome.ucsc.edu/,

473 http://hgdownload.soe.ucsc.edu/goldenPath/hg19/bigZips/hg19.fa.masked.gz). TFs
474 corresponding to transcription factor binding sequences were searched computationally
475 and manually by comparing their names and gene symbols of HGNC (HUGO Gene
476 Nomenclature Committee) -approved gene nomenclature and 31,848 UCSC known
477 canonical transcripts
478 (http://hgdownload.soe.ucsc.edu/goldenPath/hg19/database/knownCanonical.txt.gz),
479 because transcription factor binding sequences were not linked to transcript IDs such as
480 UCSC, RefSeq and Ensembl transcripts.

481 Target genes of a TF were assigned when its TFBS was found in DNase-seq
482 narrow peaks in promoter or extended regions of enhancer-promoter association of
483 genes (EPA). Promoter and extended regions were defined as follows: promoter regions
484 were those that were within distance of ±5 kb from transcriptional start sites (TSS).
485 Promoter and extended regions were defined as per the following association rule,
486 which is the same as that defined in Figure 3A of a previous study (McLean et al. 2010):
487 the single nearest gene association rule, which extends the regulatory domain to the
488 midpoint between the TSS of the gene and that of the nearest gene upstream and
489 downstream without the limitation of extension length. The limitation of extension
490 length was ＜1 Mb in this study. Extended regions for an EPA were shortened at the
491 DNA motif sites of a putative insulator TF that were the closest to a TSS, and
492 transcriptional target genes were predicted based on the shortened EPA and DNA motif
493 sites of a general TF in open chromatin regions. Promoter and extended regions of an
494 EPA were shortened at the forward–reverse (FR) orientation of DNA binding sites of a

495 putative insulator TF. When forward or reverse orientation of DNA binding sites were
496 continuously located in the genome several times, the most internal (i.e. closest to a
497 TSS) forward–reverse orientation of DNA binding sites were selected. The genomic
498 positions of genes were identified using 'knownGene.txt.gz' file in UCSC
499 bioinformatics sites (Karolchik et al. 2014). The file 'knownCanonical.txt.gz' was also
500 utilized to select representative transcripts among various alternate forms for assigning
501 promoter and extended regions of an EPA. From the list of transcription factor binding
502 sequences and transcriptional target genes, redundant transcription factor binding
503 sequences were removed by comparing the putative target genes of a transcription
504 factor binding sequence and its corresponding TF; if identical, one of the transcription
505 factor binding sequences was chosen. When the number of transcriptional target genes
506 predicted based on a transcription factor binding sequence was less than five, the
507 transcription factor binding sequence was omitted.

508 For gene expression data, RNA-seq reads mapped onto the human hg19 genome
509 sequence were obtained from UCSF-UBC human reference epigenome mapping project
510 RNA-seq reads with poly-A of naive $CD4^+$ T cells (GEO: GSM669617). For monocytes,
511 Blueprint RNA-seq FPKM data
512 ('C0010KB1.transcript_quantification.rsem_grape2_crg.GRCh38.20150622.results')
513 were downloaded from Blueprint DCC portal
514 (http://dcc.blueprint-epigenome.eu/#/files). RNA-seq reads with poly-A of human
515 mammary epithelial cells (HMEC) in Encyclopedia of DNA Elements at UCSC
516 (http://genome.ucsc.edu/encode/,

517 'wgEncodeCshlLongRnaSeqHmecCellPapAlnRep1.bam' file), H1 derived neural
518 progenitor cell (NPC) (GEO: GSM915326, ENCODE: ENCFF529SIO), Th17
519 (GSM2859479, NCBI SRA: SRR6298326), Treg (GSM2859476, SRR6298323) and
520 GM12878 (GSE78551, ENCFF297QCE) were analyzed. RNA-seq reads were aligned
521 in repeat-masked hg19 genome sequences using BWA with default parameters (Li and
522 Durbin 2009). FPKMs of the RNA-seq data were calculated by RSeQC (Wang et al.
523 2012b). Based on log2-transformed FPKM, UCSC transcripts were arranged in
524 descending order of expression level, and top 4,000 transcripts were selected in each
525 cell type.

526 The expression level of transcriptional target genes predicted based on EPAs
527 shortened at the DNA motif sites of a TF was compared with the expression level of
528 transcriptional target genes predicted based on closed chromatin regions in promoters.
529 For each DNA motif sequence shortening EPAs, transcriptional target genes were
530 predicted based on DNA binding motif sequences of vertebrate TFs in TRANSFAC
531 database, and the ratio of expression level of putative transcriptional target genes of
532 each TF was calculated between an EPA and closed chromatin regions in promoters.
533 The distribution of the ratios of all TFs was compared among forward-reverse (FR),
534 reverse-forward (RF) and non-orientation (i.e. without considering orientation) of a
535 DNA motif sequence shortening an EPA using Mann-Whitney test, two-sided (p-value <
536 10^{-7}). Other parameters for the analysis were set as follows: the number of
537 transcriptional target genes of a TF was ≥50, the number of general TFs (not insulator
538 TFs) to predict transcriptional target genes was ≥50, and the number of DNA motif

539 sites of a TF (insulator TF) shortening an EPA was ≥100.

540

541 **Comparison with chromatin interaction data**

542 For comparison of EPIs with chromatin interactions (HiChIP) in $CD4^+$ T, Th17,
543 Treg and GM12878 cells,
544 'GSM2705049_Naive_HiChIP_H3K27ac_B2T1_allValidPairs.txt',
545 'GSM2705050_Naive_HiChIP_H3K27ac_B2T2_allValidPairs.txt',
546 'GSM2705051_Naive_HiChIP_H3K27ac_B3T1_allValidPairs.txt',
547 'GSM2705054_Th17_HiChIP_H3K27ac_B1T2_allValidPairs.txt',
548 'GSM2705055_Th17_HiChIP_H3K27ac_B2T1_allValidPairs.txt',
549 'GSM2705056_Th17_HiChIP_H3K27ac_B3T1_allValidPairs.txt',
550 'GSM2705059_Treg_HiChIP_H3K27ac_B3T1_allValidPairs.txt',
551 'GSM2705041_GM_HiChIP_H3K27ac_B1_allValidPairs.txt',
552 'GSM2705042_GM_HiChIP_H3K27ac_B2_allValidPairs.txt' files were downloaded
553 from Gene Expression Omnibus (GEO) database. The resolutions of chromatin
554 interactions and EPIs were adjusted to 5 kb before their comparison. Chromatin
555 interactions with ≥6,000 and ≥1,000 counts for each interaction were analyzed in the
556 comparison in $CD4^+$ T cells. According to the unique numbers of chromatin interactions
557 in replications in Th17, Treg and GM12878 cells, chromatin interactions with ≥1,000
558 (B1T2 in Th17), ≥2,000 (B2T1 and B3T1 in Th17), ≥6,000 (B3T1 in Treg), ≥4,000
559 (B1 and B2 in GM12878) counts for each interaction were analyzed in the comparison.

560 Enhancer-promoter interactions (EPIs) were predicted based on three types of

561 EPAs in monocytes: (i) EPA shortened at the FR or RF orientation of DNA motif sites
562 of a TF, (ii) EPA shortened at the non-orientation (i.e. without considering orientation)
563 of DNA motif sites of a TF, and (iii) EPA without being shortened by a DNA motif site.
564 EPIs predicted based on the three types of EPAs in common were removed. EPIs
565 predicted based on EPA (i) were removed from EPIs predicted based on EPA (ii). EPIs
566 predicted based on EPA (i) and (ii) were removed from EPIs predicted based on EPA
567 (iii). The resolution of HiChIP chromatin interaction data was 1-5 kb, so EPIs were
568 adjusted to 5 kb before their comparison. The number and ratio of EPIs overlapped with
569 chromatin interactions were compared two times between EPI (i) and (iii), and EPI (i)
570 and (ii) (binomial distribution, p-value < 0.025 for each test, two-sided, 95% confidence
571 interval).

572 For comparison of EPIs with chromatin interactions (in situ Hi-C) in HMEC, the
573 genomic positions of chromatin interactions in 'HMEC_4DNFI97O9SAZ.pairs.gz' file
574 in 4D nucleome data portal (http://data.4dnucleome.org) were converted into hg19
575 version of human genome using liftOver tool
576 (http://hgdownload.soe.ucsc.edu/downloads.html#liftover). The resolutions of
577 chromatin interaction data and EPIs were adjusted to 3 kb before their comparison. All
578 chromatin interactions were used in the comparison. For comparison of EPIs with
579 chromatin interactions (promoter capture Hi-C) in NPC, the resolutions of chromatin
580 interaction data in 'GSE86189_npc.po.all.txt.bz2' file (GEO: GSE86189) and EPIs were
581 adjusted to 5 kb before their comparison. All chromatin interactions were used in the
582 comparison.

583 Putative target genes for the comparison of EPIs and chromatin interactions were
584 selected from top 4,000 transcripts in term of the expression level. The expression level
585 of putative target genes of EPIs overlapped with chromatin interactions was compared
586 with EPIs not overlapped with them. When the same transcriptional target gene of a TF
587 in an enhancer was predicted based on both an EPI overlapped with a chromatin
588 interaction and an EPI not overlapped with, the target gene was eliminated. The
589 distribution of expression level of putative target genes was compared using
590 Mann-Whitney test, two-sided (p-value < 0.05).
591
592 **Correlation of expression level of gene pairs separated by DNA motif sites of a TF**
593 To examine the correlation of expression level of genes pairs separated by DNA
594 motif sites of a TF, gene expression data among 53 tissues were obtained from
595 'GTEx_Analysis_2016-01-15_v7_RNASeQCv1.1.8_gene_median_tpm.gct.gz' file in
596 GTEx database (https://gtexportal.org/home/). The correlation of log2-transformed gene
597 expression level was analyzed based on protein-coding transcripts of RefSeq (RefSeq
598 ID with 'NM_'). The same genomic location of RefSeq transcripts were removed. DNA
599 motif sites overlapped with RefSeq transcripts were eliminated. Genes closest to a DNA
600 motif sites and another gene were analyzed using BEDOPS closest-features (Neph et al.
601 2012). Mann-Whitney test was performed using R.
602
603 ## Acknowledgements
604 The supercomputing resource was provided by Human Genome Center of the Institute

605 of Medical Science at the University of Tokyo. Publication charges for this article were
606 funded by JSPS KAKENHI Grant Number 16K00387. This work was partially
607 supported by JST CREST Grant Number JPMJCR15G1, Japan.
608

609 **Figures**

610 Web links to original figures.

611 Figure 1. (A) Figure 1. Enhancers and their features. (Shlyueva et al. 2014)

612 https://static-content.springer.com/esm/art%3A10.1038%2Fnrg3682/MediaObjects/415

613 76_2014_BFnrg3682_MOESM18_ESM.ppt

614 Graphical Abstract (de Wit et al. 2015)

615 https://marlin-prod.literatumonline.com/cms/attachment/7d219941-8398-4373-9ac9-8bf

616 92c5eba1d/fx1.jpg

617

618 (B) Supplementary Figure 2. Computationally-defined regulatory domain (McLean et al.

619 2010)

620 https://static-content.springer.com/esm/art%3A10.1038%2Fnbt.1630/MediaObjects/415

621 87_2010_BFnbt1630_MOESM11_ESM.pdf

622 Figure 4. The Role of CBS Location and Orientation in CTCF-Mediated Genome-wide

623 DNA Looping (Guo et al. 2015)

624 https://marlin-prod.literatumonline.com/cms/attachment/297a06ad-7568-483e-9904-9ae

625 2af081251/gr4.jpg

626

627 **Figure 1.** Chromatin interaction and enhancer-promoter association. (A) Forward–

628 reverse orientation of CTCF-binding sites are frequently found in chromatin interaction

629 anchors. CTCF can block the interaction between enhancers and promoters limiting the

630 activity of enhancers to certain functional domains (Rao et al. 2014; Shlyueva et al.

631 2014; de Wit et al. 2015; Guo et al. 2015). (B) Computationally-defined regulatory
632 domains for enhancer-promoter association (McLean et al. 2010). The *single nearest*
633 *gene* association rule extends the regulatory domain to the midpoint between this gene's
634 TSS and the nearest gene's TSS both upstream and downstream. The enhancer-promoter
635 association was shortened at the forward-reverse orientation of DNA binding motif sites
636 of a TF in this study (e.g. CTCF in the figure).
637

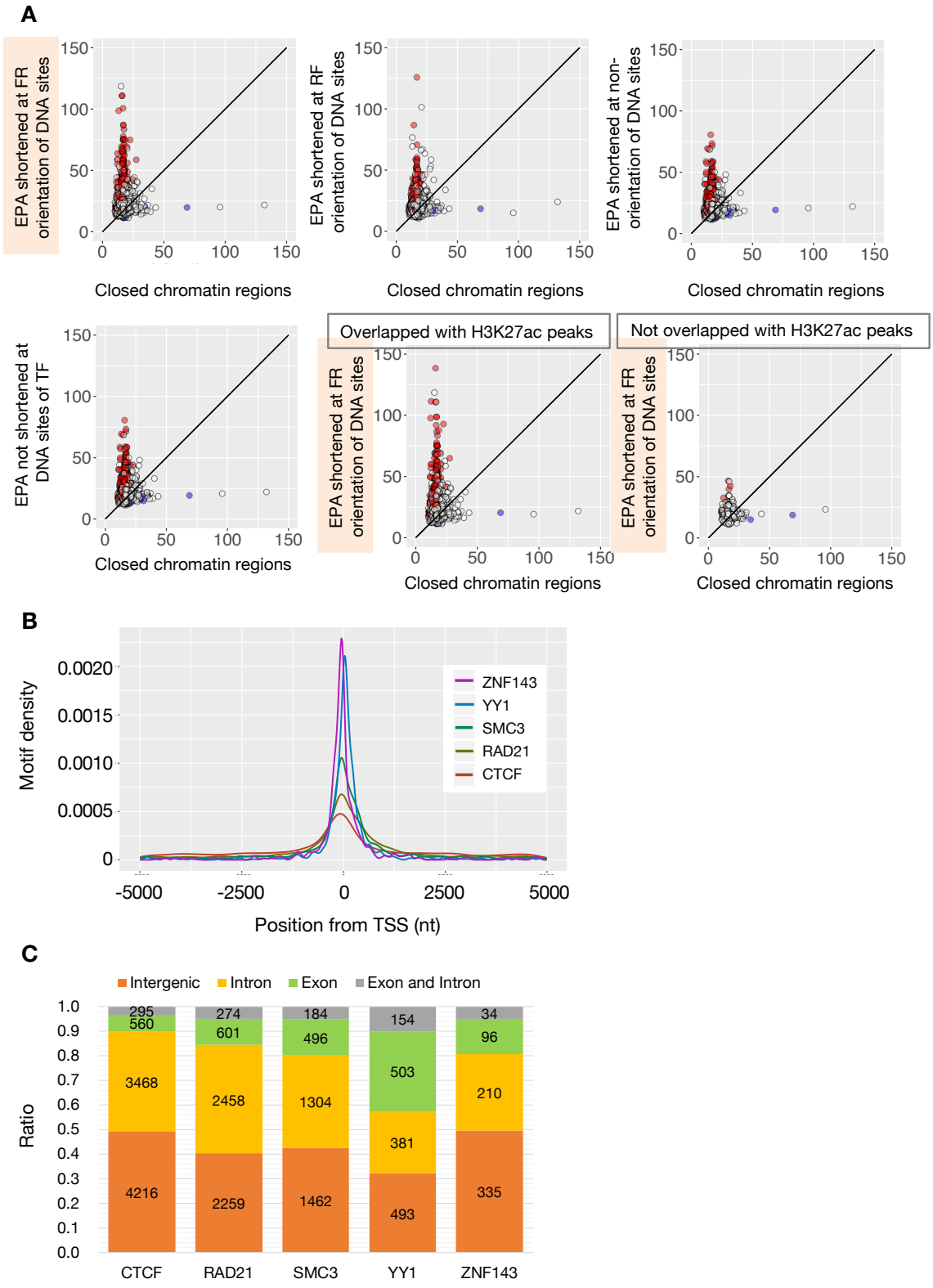

Figure 2. Identification of DNA motif sites of TFs in open chromatin regions and properties of DNA motif sites of TFs. (A) Comparison of expression level of putative

641 transcriptional target genes. Each dot represents the median expression level (FPKM) of
642 target genes predicted based on DNA motif sites of a transcription factor in closed
643 chromatin regions in promoters (X-axis) and an enhancer-promoter association (EPA)
644 shortened at the forward-reverse orientation of DNA motif sites of CTCF (Y-axis) in T
645 cell (upper left graph). The distribution of expression level was changed according to
646 four criteria of EPAs (four graphs) (Osato 2018). Red dots indicate the median
647 expression level of target genes was significantly higher in an EPA than closed
648 chromatin regions, and blue dots indicate the median expression level of target genes
649 was significantly lower in an EPA than closed chromatin regions (Mann-Whitney test).
650 The expression level of target genes predicted based on an EPA tend to be higher than
651 closed chromatin regions, implying that TFs serve as activators of target genes. DNA
652 motif sites of TFs overlapped with H3K27ac ChIP-seq peaks were associated with a
653 significant difference of expression level of target genes, and DNA motif sites not
654 overlapped with H3K27ac peaks were not associated with the difference (lower right
655 two graphs). This suggests that the significant difference of expression level is
656 associated with enhancer (and promoter) signals of H3K27ac. (B) Distribution of DNA
657 motif sites of TFs near TSS. ZNF143 and YY1 tend to be located near TSS, and CTCF
658 tend to be observed more in distant regions than around TSS in monocyte. (C)
659 Distribution of DNA motif sites of TFs in the human genome in monocytes. Most of
660 DNA motif sites were found in intergenic and intron regions. YY1 is known to be at
661 TSS in the edge of exons of genes, and is involved in transcriptional activation,
662 repression and initiation.

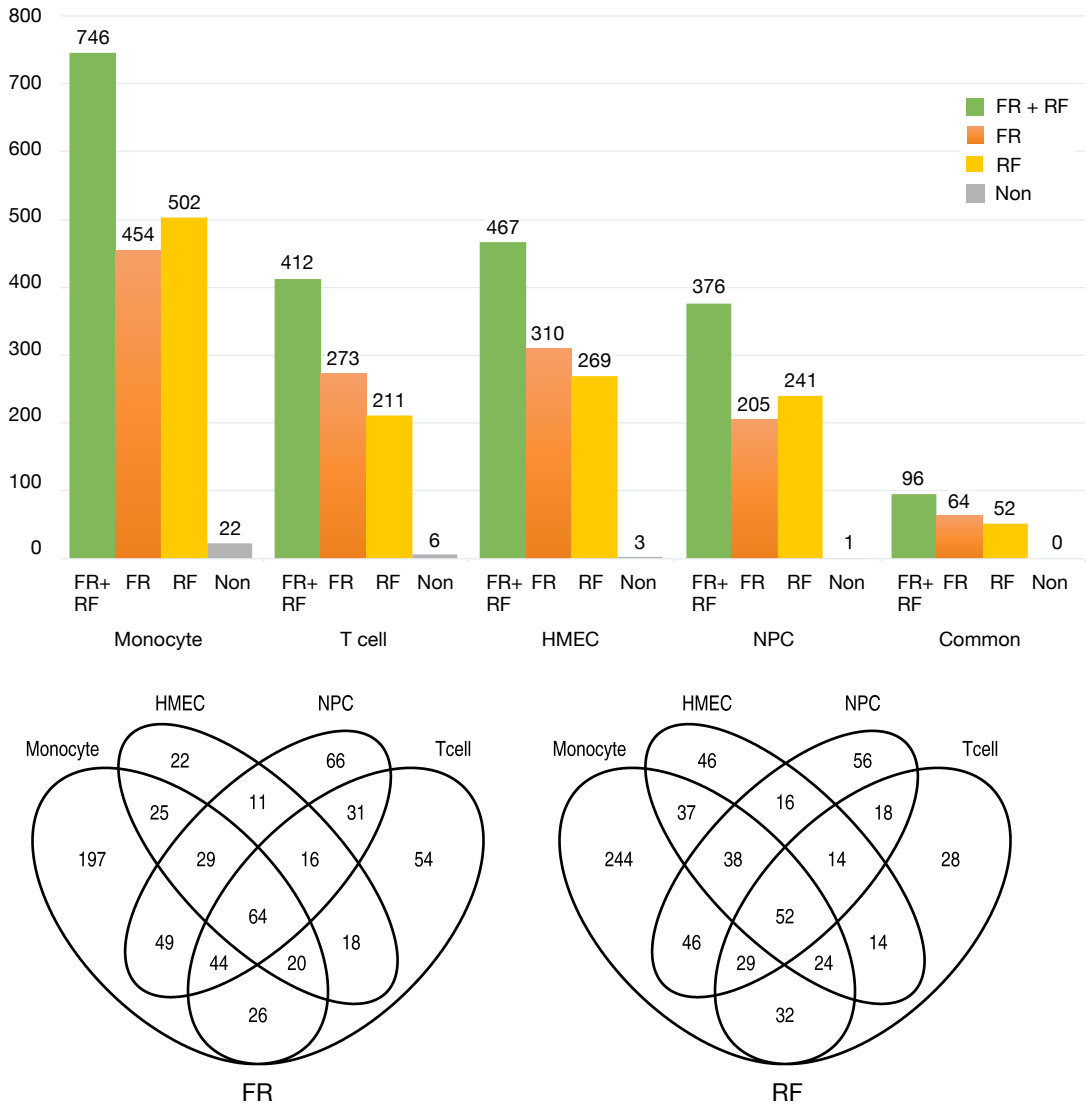

Figure 3. Biased orientations of DNA motif sequences of TFs affect the transcription of genes by the putative insulator function of the DNA motif sites. Total 96 (64 FR and 52 RF) of biased orientations of DNA binding motif sequences of TFs affected significantly the expression level of putative transcriptional target genes in monocytes, T cells, HMEC and NPC in common, whereas non-orientation (i.e. without considering

670 orientation) of DNA binding motif sequence of a TF did not affect the expression level

671 significantly.

672

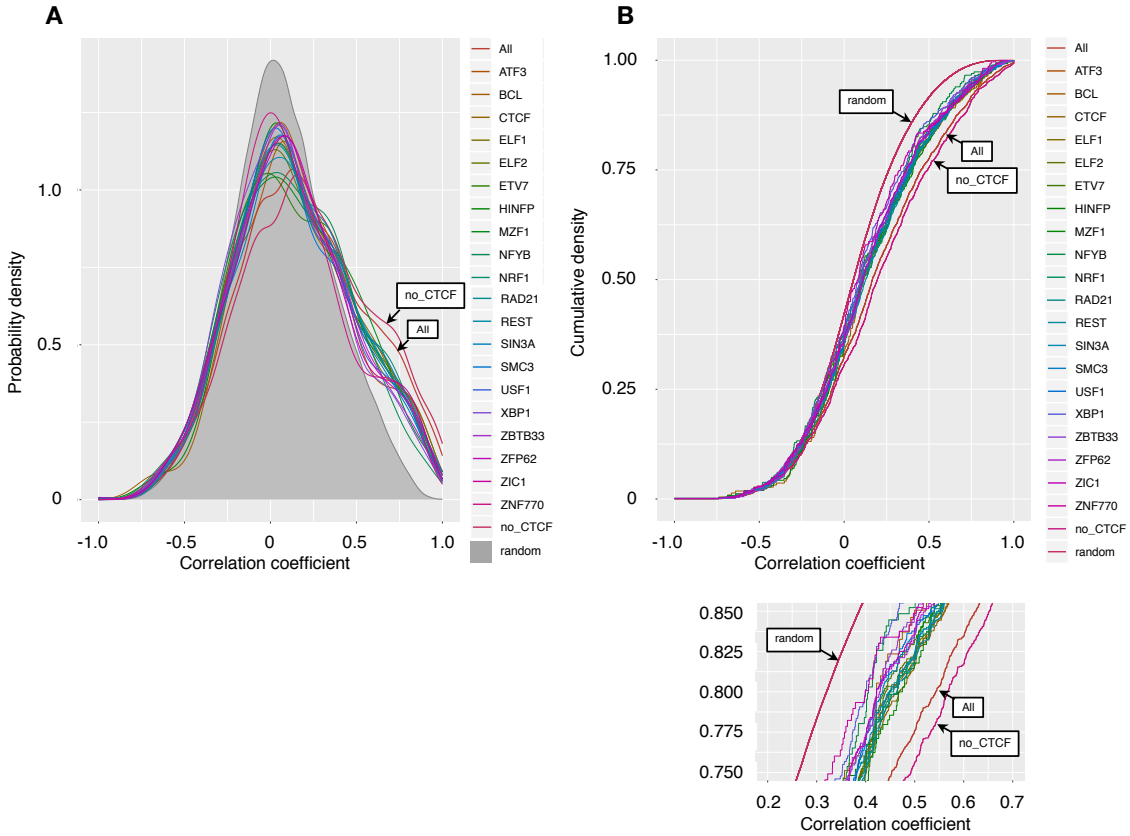

673

674 **Figure 4.** Genes separated by predicted DNA binding sites of biased orientations of

675 DNA motifs of TFs are less correlated in gene expression. Top 20 TFs are selected

676 according to ascending order of median correlation coefficient. Correlation coefficient

677 between neighboring gene pairs is shown in terms of probability density (A) and

678 cumulative distribution (B). Brown line (All), correlation between all neighboring

679 genes; gray shading in (A) and red line (random) in (B), correlation between randomly

680 chosen gene pairs; Purple line (no_CTCF), correlation between gene pairs not separated

681 by predicted CTCF sites.

682 Web links to original figures.

683 Figure 5. Schematic representation of chromatin interactions involving gene promoters

684 (Bailey et al. 2015).

685 https://www.nature.com/articles/ncomms7186/figures/5

686

687 **Figure 5.** Schematic representation of chromatin interactions involving gene promoters.

688 ZNF143 contributes the formation of chromatin interactions by directly binding the

689 promoter of genes establishing looping with distal element bound by CTCF (Bailey et al.

690 2015).

691

692

Tables

Table 1. Biased orientations of DNA binding motif sequences of TFs in monocytes, T cells, HMEC and NPC in common. TF: DNA binding motif sequences of transcription factors.

Forward-reverse orientation

TF	P-value
AHR	0
ARNT	0
ARNTL	7.96E-08
ATF2	3.09E-14
ATF3	2.22E-15
BCL	0
BHLHE41	5.55E-14
CREB3L1	0
CTCF	0
CXXC1	0
E2F	0
E2F1	0
EGR1	0
EGR3	0
EGR4	0
ELF1	0
ELF2	5.74E-13
ELK3	3.33E-15
ELK4	6.19E-11
ERG	0
ETS	0
ETS1	0
ETV7	2.31E-08
HEY2	0
HIC1	0
HINFP	6.46E-14
INSM1	2.22E-16
KLF4	0
KLF7	9.07E-09
MAX	0

TF	P-value
MYC	0
MYCN	0
MZF1	0
NFY	1.72E-11
NFYB	0
NONO	0
NRF1	1.63E-11
OVOL2	0
PLAG1	0
PLAGL1	0
RAD21	0
REST	0
RFX1	0
SIN3A	0
SIX5	0
SMC3	0
SP2	1.04E-11
TFAP2A	0
TFAP2B	2.22E-16
TFAP2C	0
TP73	0
USF1	0
XBP1	0
YY1	0
YY2	0
ZBTB33	0
ZBTB7A	0
ZFP62	0
ZFX	0
ZIC1	0

TF	P-value
ZNF143	0
ZNF740	0
ZNF770	6.51E-08
ZNF84	0

Reverse-forward orientation

TF	P-value
AP1	0
ARNT	1.26E-11
ATF3	0
BHLHE40	8.88E-16
CREB1	0
CTCF	0
E2F	2.32E-13
E2F3	0
EFNA2	6.61E-11
EGR1	0
EGR2	0
ETS1	0
FLI1	1.05E-13
FLI1:FIGLA	0
FOS	0
GMEB2	0
HIF1A	0
KLF4	0
MITF	0
MYB	0
MYC	0
MYCN	0
MZF1	0
NFKB1	0
NFYA	2.31E-13
NR3C1	0
NRF1	0
OSR2	0
PBX3	0
PLAG1	2.78E-14

TF	P-value
RFX2	0
RFX5	0
RUNX3	0
SP1	0
SP2	0
SP4	0
SPDEF	0
SREBF2	0
STAT	0
TATA	0
TFAP2B	2.00E-15
TFAP2C	0
TFCP2L1	0
USF1	7.55E-10
YBX1	0
YY1	0
YY2	0
ZBTB33	0
ZBTB7B	0
ZNF100	6.22E-14
ZNF143	0
ZNF432	0

701 **Table 2.** Comparison of enhancer-promoter interactions (EPIs) with chromatin
702 interactions in T cells. The upper tables show the number of biased orientations of DNA
703 motifs, where a significantly higher ratio of EPIs that were predicted based on an
704 enhancer-promoter association (EPA) (i) overlapped with HiChIP chromatin
705 interactions than the other types of EPA (ii) and (iii) in T cells. The middle tables show
706 133 FR and 90 RF orientations of DNA motifs found in common among B2T1, B2T2
707 and B3T1 replications in T cells in the upper table. The lower tables show that among
708 64 FR and 52 RF orientations of DNA motifs found in common in monocytes, T cell,
709 HMEC and NPC, 44 (69%) FR and 28 (54%) RF were matched with the analysis of
710 HiChIP chromatin interactions according to three types of EPAs. TF: DNA binding
711 motif sequence of a transcription factor. Score: $-\log_{10}$ (*p*-value). Score 1: Comparison of
712 an EPA shortened at the FR or RF orientation of DNA motif sites [EPA (i)] with an EPA
713 not shortened [EPA (iii)]. Score 2: Comparison of an EPA shortened at the FR or RF
714 orientation of DNA motif sites [EPA (i)] with an EPA shortened at the non-orientation of
715 DNA motif sites [EPA (ii)].

1. Comparison of EPI with HiChIP data among three EPA (i), (ii) and (iii)

Replication of HiChIP data	Total no. (FR + RF) of DNA motifs	No. of FR DNA motifs	No. of RF DNA motifs
B2T1	226	153	101
B2T2	221	149	98
B3T1	237	160	109
DNA motifs found in common among replications			
B2T1 and B2T2	212	141	95
B2T1 and B3T1	212	143	93
B2T2 and B3T1	208	138	93
B2T1, B2T2 and B3T1	201	133	90

2. Comparison of EPI with HiChIP data between two EPA (i) and (iii)

Replication of HiChIP data	Total no. (FR + RF) of DNA motifs	No. of FR DNA motifs	No. of RF DNA motifs
B2T1	395	262	205
B2T2	398	264	204
B3T1	394	263	203
DNA motifs found in common among replications			
B2T1 and B2T2	394	262	202
B2T1 and B3T1	391	261	202
B2T2 and B3T1	392	262	200
B2T1, B2T2 and B3T1	390	261	199

FR and RF orientations of DNA motifs found in common among three replications in T cell.

Forward-reverse (FR)

TF	Score 1	Score 2	TF	Score 1	Score 2	TF	Score 1	Score 2
AHR	38.81	13.41	ETS2	208.78	13.99	MNT	215.63	8.00
ARNTL	155.78	1.96	ETV1	153.32	7.02	MTF1	323.31	14.21
ATF1	323.31	15.00	ETV3	140.11	14.58	MXI1	323.31	70.98
ATF3	323.31	35.22	ETV5:EVX1	145.48	17.33	MYC	84.79	24.93
BCL	153.72	3.52	ETV5:HES7	8.76	8.74	MYCN	165.16	25.87
CREB	90.91	2.32	ETV5:TCF3	203.52	5.90	MZF1	81.83	2.29
CREB3	323.31	38.74	FOXN4	73.43	5.59	NFKB1	279.24	14.27
CREB3L1	323.31	27.96	FOXO1:ELK3	323.31	43.51	NFKB1:NFKB1	323.31	13.79
CTCF	323.31	3.50	GABPA	197.57	20.39	NFY	323.31	3.42
CTCFL	174.90	2.09	GABPA:GABPB1	142.28	6.10	NONO	323.31	9.24
CXXC1	69.92	3.30	GCM2	13.68	18.80	NR2C2	323.31	3.64
E2	323.31	20.15	GDNF	286.73	3.15	NRF1	45.13	30.75
E2F	122.12	21.87	GMEB1	136.68	10.56	OVOL2	323.31	31.61
E2F1	43.22	2.85	HIC1	223.55	4.56	PATZ1	101.85	9.30
EGR1	79.09	3.79	HIF1A	241.47	1.71	PLAG1	177.90	11.02
EGR2	176.69	4.53	HOXB2:ETV1	102.22	2.42	PURA	196.04	17.98
EGR3	85.25	34.18	ID2	323.31	14.52	R	22.49	3.99
EHF	323.31	8.66	INSM1	193.85	15.87	**RAD21**	258.21	4.81
ELF1	203.38	3.86	JUN:JUNB	275.78	6.48	RBAK	267.43	11.25
ELF2	227.62	7.83	JUNB:JUN	202.73	5.07	RELA	323.31	4.68
ELF5	323.31	8.76	KLF	252.10	8.35	RFX1	159.78	17.05
ELK1:TBX21	126.46	8.41	KLF15	323.31	22.56	RFX4	323.31	35.28
ELK1:TEF	323.31	7.99	KLF17	87.51	14.77	RFX5	323.31	26.52
ELK4	117.83	4.81	KLF2	90.74	15.34	SAP1	124.23	14.63
ENO1	80.42	3.13	KLF4	209.71	9.38	**SMC3**	222.09	1.76
EPAS1	65.43	7.76	KLF7	229.95	11.96	SP1	235.48	29.09
ERF	207.67	6.25	LHX8	244.38	2.95	SP2	94.11	9.54
ERG	199.81	25.70	MAX	323.31	8.35	SP4	14.30	6.31
ETS	196.80	1.63	MAZ	109.42	3.37	SPDEF	179.39	16.81
ETS1	308.00	3.92	MBD2	8.41	1.95	SPIC	323.31	28.49

TF	Score 1	Score 2
STAT	84.60	1.69
STAT1	323.31	5.38
TCF12	111.44	16.79
TCF3	323.31	14.05
TEAD4:ETV4	226.28	5.90
TFAP2A	25.86	20.26
TFAP2B	90.03	6.10
TFAP2C	169.60	8.55
TFAP4	93.98	2.36
TFE3	139.21	16.71
TP73	198.45	7.75
TR4	39.01	4.97
USF1	194.06	3.56
VEZF1	134.36	3.49
XBP1	323.31	44.58
XRCC5:XRCC6	132.56	3.92
YY1	62.59	5.30
ZBED6	183.14	20.23
ZBTB17	48.37	7.27
ZBTB26	151.91	16.84
ZBTB5	120.19	9.58
ZBTB7A	52.89	30.58
ZFX	13.33	14.55
ZFY	36.57	4.04
ZIC3	266.75	10.54
ZIC4	17.27	9.30
ZNF140	323.31	4.99
ZNF143	323.31	35.38
ZNF165	323.31	7.80
ZNF25	281.69	7.72

TF	Score 1	Score 2
ZNF322	120.49	11.55
ZNF325	69.42	2.74
ZNF408	214.73	2.22
ZNF467	127.21	4.64
ZNF479	226.76	3.26
ZNF48	106.17	9.88
ZNF511	84.74	9.87
ZNF553	93.45	9.17
ZNF555	232.83	7.63
ZNF624	235.50	3.84
ZNF672	266.64	10.80
ZNF675	323.31	5.81
ZNF676	323.31	16.54

Reverse-forward (RF)

TF	Score 1	Score 2
ARNT	323.31	14.12
ARNT2	41.41	42.78
ASCL2	138.15	6.41
ATF3	323.31	14.64
ATF4	323.31	25.14
ATF7	79.30	4.96
BCLAF1	148.24	8.52
BHLHE40	323.31	12.42
CDCA7L	84.72	8.42
CREB3	206.55	11.07
CREB3L1	323.31	7.63
CREB3L2	67.51	7.98
CTCF	240.61	4.56
E2F	78.16	7.07
E2F1	124.10	15.73
E2F3	65.67	8.85
E2F6	165.75	30.69
EFNA2	255.01	10.95
ELK3	143.48	7.57
EP300	121.01	10.90
ETV5:CLOCK	42.10	7.29
GLIS2	37.40	17.34
GMEB2	323.31	7.81
HES1	88.18	9.46
HES7	166.52	14.60
HIVEP1	323.31	4.90
HOXB2:ELK1	217.94	11.92
IRC900814	323.31	4.89
KLF4	213.35	9.49
KLF8	323.31	17.42

TF	Score 1	Score 2
MAX	304.34	8.64
MLXIPL	64.44	10.74
MUSCLE	23.05	3.47
MYB	323.31	17.68
MYBL1	316.23	23.27
MYC	323.31	12.23
MZF1	200.49	22.73
NFY	209.97	3.22
NFYA	323.31	11.75
NHLH1	105.19	4.42
NR1H3	323.31	9.38
NR3C1	43.16	8.31
OSR2	111.77	14.65
RFX1	323.31	22.99
RXRA	146.30	15.11
SALL1	277.84	1.91
SCRT2	301.48	9.60
SMAD6	259.24	7.43
SP100	20.75	7.99
SP2	294.86	2.59
SP4	110.94	19.63
SPDEF	185.85	14.35
SPZ1	323.31	9.87
SREBF1	67.27	15.74
SREBF2	297.27	1.62
TAF1	252.27	17.47
TATA	2.16	4.02
TFAP2A	20.17	29.15
TFAP2B	29.46	12.62
TFAP2C	112.10	51.21

TF	Score 1	Score 2
TFE3	95.23	10.59
THAP1	127.72	5.07
YY1	323.31	9.92
YY2	47.49	2.61
ZBTB33	90.29	7.78
ZBTB45	323.31	57.08
ZBTB7A	89.19	16.19
ZBTB7B	43.90	23.59
ZFP64	147.00	13.59
ZIC3	42.65	15.39
ZNF100	27.67	4.75
ZNF143	63.03	9.69
ZNF148	213.77	18.93
ZNF16	323.31	47.43
ZNF37A	310.67	14.79
ZNF410	140.45	13.57
ZNF419	247.63	11.25
ZNF429	87.05	32.39
ZNF436	323.31	11.48
ZNF468	21.12	7.67
ZNF557	299.44	9.58
ZNF575	39.45	14.38
ZNF586	260.73	6.18
ZNF611	279.80	15.65
ZNF616	189.53	30.98
ZNF692	202.47	2.33
ZNF727	214.01	17.22
ZNF770	300.52	4.71
ZNF773	150.45	8.84
ZSCAN21	323.31	5.55

FR and RF orientations of DNA motifs found in common in the four cell types.

Forward-reverse (FR)

TF	Score 1	Score 2
AHR	38.81	13.41
ARNTL	155.78	1.96
ATF3	323.31	35.22
BCL	153.72	3.52
CREB3L1	323.31	27.96
CTCF	323.31	3.50
CXXC1	69.92	3.30
E2F	122.12	21.87
E2F1	43.22	2.85
EGR1	79.09	3.79
EGR3	85.25	34.18
ELF1	203.38	3.86
ELF2	227.62	7.83
ELK4	117.83	4.81
ERG	199.81	25.70
ETS	196.80	1.63
ETS1	308.00	3.92
HIC1	223.55	4.56
INSM1	193.85	15.87
KLF4	209.71	9.38
KLF7	229.95	11.96
MAX	323.31	8.35
MYC	84.79	24.93
MYCN	165.16	25.87
MZF1	81.83	2.29
NFY	323.31	3.42
NONO	323.31	9.24
NRF1	45.13	30.75
OVOL2	323.31	31.61
PLAG1	177.90	11.02

TF	Score 1	Score 2
RAD21	258.21	4.81
RFX1	159.78	17.05
SMC3	222.09	1.76
SP2	94.11	9.54
TFAP2A	25.86	20.26
TFAP2B	90.03	6.10
TFAP2C	169.60	8.55
TP73	198.45	7.75
USF1	194.06	3.56
XBP1	323.31	44.58
YY1	62.59	5.30
ZBTB7A	52.89	30.58
ZFX	13.33	14.55
ZNF143	323.31	35.38

Reverse-forward (RF)

TF	Score 1	Score 2
ARNT	323.31	14.12
ATF3	323.31	14.64
BHLHE40	323.31	12.42
CTCF	240.61	4.56
E2F	78.16	7.07
E2F3	65.67	8.85
EFNA2	255.01	10.95
GMEB2	323.31	7.81
KLF4	213.35	9.49
MYB	323.31	17.68
MYC	323.31	12.23
MZF1	200.49	22.73
NFYA	323.31	11.75
NR3C1	43.16	8.31
OSR2	111.77	14.65
SP2	294.86	2.59
SP4	110.94	19.63
SPDEF	185.85	14.35
SREBF2	297.27	1.62
TATA	2.16	4.02
TFAP2B	29.46	12.62
TFAP2C	112.10	51.21
YY1	323.31	9.92
YY2	47.49	2.61
ZBTB33	90.29	7.78
ZBTB7B	43.90	23.59
ZNF100	27.67	4.75
ZNF143	63.03	9.69

Table 3. Correlation of expression level of gene pairs separated by DNA motif sites of a TF. Pairs of genes separated by 64 FR and 52 RF orientations of DNA motif sites of TFs found in common in monocytes, T cells, HMEC and NPC were analyzed to find significantly lower correlation of their expression level than the correlation of all pairs of nearby genes among 53 tissues. Score: $-\log_{10}$ (p-value) of Mann-Whitney test. Median correlation: median correlation coefficient of expression level of nearby gene pairs separated by DNA motif sites. The median correlation coefficient of expression level of all pairs of nearby genes is 0.17. # DNA site: number of DNA motif sites of a

740 TF separating gene pairs with expression data. All DNA motif sites of a TF were used,
741 except for DNA motif sites separating pairs of ubiquitously expressed genes with
742 coefficient of variance <90.

743

744 Forward-reverse (FR)

TF	Score	Median correlation	# DNA site
AHR	1.80	0.12	520
ARNT	1.35	0.09	141
ATF2	1.40	0.11	166
ATF3	3.61	0.11	795
BHLHE41	2.02	0.07	118
CREB3L1	2.88	0.05	127
CTCF	6.02	0.09	837
E2F	3.73	0.10	444
E2F1	3.79	0.11	868
EGR1	2.97	0.10	391
ELF1	4.86	0.10	714
ELF2	3.88	0.11	781
ELK3	1.86	0.12	547
ELK4	2.44	0.11	663
ETS	3.34	0.11	523
ETS1	4.27	0.11	687
ETV7	3.68	0.11	662
HIC1	1.65	0.11	380
HINFP	1.33	0.09	258
KLF4	2.00	0.13	718
MYC	3.86	0.11	762
MYCN	2.36	0.11	583
MZF1	1.74	0.10	261
NFYB	2.97	0.10	264
NRF1	2.21	0.11	640
PLAG1	2.93	0.10	503
PLAGL1	2.55	0.10	414
RAD21	6.08	0.09	852
REST	4.35	0.11	920
RFX1	2.38	0.08	81
SIN3A	3.31	0.11	813
SMC3	6.18	0.09	625
SP2	2.30	0.12	738
TFAP2A	4.17	0.11	767
TFAP2C	2.13	0.11	470
USF1	4.24	0.10	628
XBP1	6.65	0.07	379
ZBTB33	4.90	0.10	701
ZBTB7A	2.82	0.10	485
ZFP62	2.95	0.11	565
ZFX	2.69	0.11	581
ZIC1	4.47	0.11	829
ZNF770	3.38	0.08	271

Reverse-forward (RF)

TF	Score	Median correlation	# DNA site
AP1	3.87	0.11	744
ARNT	2.95	0.10	453
ATF3	4.34	0.10	665
BHLHE40	2.49	0.07	155
CREB1	1.79	0.11	303
CTCF	5.96	0.09	721
E2F	3.95	0.10	663
E2F3	4.05	0.09	616
EFNA2	3.51	0.10	543
EGR1	2.58	0.10	428
EGR2	1.39	0.13	747
ETS1	3.75	0.11	667
FLI1:FIGLA	5.41	0.08	428
FOS	3.51	0.11	777
GMEB2	1.36	0.09	310
HIF1A	2.34	0.11	448
KLF4	2.21	0.12	744
MITF	3.14	0.10	419
MYC	4.85	0.10	704
MYCN	2.79	0.10	507
NFKB1	1.59	0.11	342
NFYA	2.15	0.10	229
NRF1	2.01	0.12	615
OSR2	1.99	0.12	301
PBX3	2.20	0.11	253
RFX2	2.12	0.09	168
RFX5	3.03	0.05	75
RUNX3	2.01	0.11	241
SP1	2.73	0.11	725
SP2	2.15	0.12	1090
SP4	2.33	0.11	479
SPDEF	5.29	0.07	449
TFAP2B	3.42	0.11	855
TFAP2C	2.05	0.11	576
TFCP2L1	1.45	0.13	362
YBX1	1.34	0.13	160
YY1	2.23	0.01	50
ZBTB33	3.44	0.11	886
ZBTB7B	2.27	0.13	892
ZNF143	2.26	0.07	81

745

Table 4. Top 30 of co-location and overlapping biased orientations of DNA binding motif sequences of TFs in monocytes. Co-location and overlapping DNA motif sequences of CTCF with another biased orientation of DNA motif sequence are shown in separate tables. Motif 1,2: DNA binding motif sequences of TFs. No.: the number of genomic locations with both Motif 1 and Motif 2 in upstream and downstream of genes in an EPA (< 1 Mb distance from TSS of genes). Total number of genes is 30,523.

Forward-reverse (FR)

Motif 1	Motif 2	No.	Mean of distances bet. DNA sites (nt)	Median of distances bet. DNA sites (nt)	Mean of distances from TSS (nt)	Median of distances from TSS (nt)	Interquartile range of distance from TSS (nt)
FOS	JUN	3332	0.00	0	43202.95	18085	5524 - 48583
CTCF	**SMC3**	2876	0.01	0	34606.92	13716	3073 - 39471
FOSL2	JUN	2807	0.00	0	40389.84	17365	5424 - 45251
FOSB	FOSL2	2644	0.00	0	44302.93	17867	5633 - 47209
EGR1	EGR2	2397	0.00	0	14578.21	1251	247 - 11473
CTCF	**RAD21**	2352	0.00	0	33492.68	12913	2824 - 37672
RAD21	**SMC3**	2343	0.02	0	33572.80	14302	3856 - 37159
ATF3	FOSL2	2322	0.00	0	42784.04	17841	5366 - 48236
FOSL2	JUNB	2305	0.02	0	42884.36	17867	5706 - 46515
ETS2	ETSLIKE	2205	0.00	0	37660.66	15765	4146 - 41462
FOS	JUNB	2151	0.00	0	38403.20	16367	4849 - 44736
IRF	IRF4	1962	0.00	0	40794.41	15872	3969 - 45946
FOSL2	SMARCC1	1945	0.00	0	42429.69	17369	5094 - 46586
EGR1	WT1	1941	0.16	0	12485.23	427	93 - 5394
FOSB	JUN	1808	0.02	0	36648.74	16705	5156 - 40309
ATF3	JUN	1713	0.02	0	38101.24	17119	5294 - 43559
JUN	TFAP2A	1628	0.00	0	42262.97	18017	5089 - 47094
FOSL2	TFAP2A	1628	0.00	0	36606.38	16201	4949 - 41948
BACH2	SMARCC1	1462	0.16	0	38673.02	14778	4060 - 41262
ELF1	ETS1	1459	0.00	0	37056.72	14346	3370 - 40339
CHD2	E2F	1429	0.00	0	19220.38	1579	329 - 16257
JUN	NR3C1	1262	0.00	0	35052.17	14418	3844 - 38534
USF1	USF2	1260	0.00	0	25188.91	4726	413 - 24699
BACH2	JUNB	1238	0.15	0	36252.37	15302	4462 - 39393
BACH2	FOSB	1184	0.22	0	37190.80	14778	4038 - 41262
ETSLIKE	GABPA	1164	0.00	0	32352.24	11683	2356 - 36919
CTCF	CTCFL	1151	0.00	0	30252.04	11606	2229 - 34539
NR5A1	NR5A2	1133	0.00	0	41171.86	12243	2488 - 43136
ATF3	BACH2	1094	0.18	0	35659.16	13605	3821 - 39756
ETS2	GABPA	1092	0.06	0	27250.24	12184	2858 - 32196

Reverse-forward (RF)

Motif 1	Motif 2	No.	Mean of distances bet. DNA sites (nt)	Median of distances bet. DNA sites (nt)	Mean of distances from TSS (nt)	Median of distances from TSS (nt)	Interquartile range of distance from TSS (nt)
EGR1	EGR3	3012	0.00	0	17005.00	709	149 - 10393
NR1I2	NR1I3	2932	0.00	0	49622.84	20548	5924 - 58436
ZIC1	ZIC3	2871	0.07	0	21511.64	3092	434 - 19128
EGR	WT1	2612	0.04	0	9949.38	396	102 - 4266
FOS	FOS:JUN	2512	0.01	0	37200.80	15466	4438 - 42373
EGR	EGR3	2293	0.17	0	11634.92	532	135 - 6044
MAFG	NFE2L1:MAFG	2272	0.03	0	34641.56	16917	5284 - 42097
KLF10	SP1	2233	0.00	0	9778.94	297	73 - 3077
EGR	EGR2	2160	0.16	0	10502.76	490	129 - 5227
KLF3	SP3	2036	0.00	0	6974.78	246	63 - 1447
KLF1	SP3	1771	0.00	0	7748.42	264	66 - 1829
KLF10	SP3	1734	0.00	0	7275.48	222	58 - 1320
KLF7	SP4	1639	0.00	0	12521.62	309	58 - 4894
KLF1	SP1	1574	0.05	0	6780.46	245	61 - 1438
AP1	JUNB	1572	0.05	0	34158.07	15451	4746 - 40315
EGR1	WT1	1543	0.31	0	12742.28	444	111 - 5553
EGR1	SP1:SP3	1393	0.08	0	7789.54	307	91 - 1886
FOS:JUN	JUNB	1386	0.14	0	33012.80	14245	3900 - 37988
SP1	SP3	1372	0.00	0	8845.31	293	77 - 1816
EHF	ELF1	1366	0.02	0	41217.39	13357	2842 - 43178
CTCF	RXRA	1362	0.00	0	29981.33	10937	2100 - 31407
AP1	FOS	1327	0.03	0	33225.52	13455	3503 - 37399
ATF1	ATF3	1215	0.00	0	23125.06	3798	342 - 21091
ELK1	ZNF200	1156	0.05	0	22200.49	2883	181 - 17610
SP1	SP4	1137	0.00	0	7371.85	215	63 - 1232
EHF	ELF3	1134	0.00	0	36296.46	10912	596 - 37318
MEIS2	TGIF1	1018	0.00	0	47677.15	17654	3273 - 49233
KLF3	SP1	1017	0.06	0	6514.33	226	60 - 994
SPI1	ZNF200	913	0.06	0	10962.81	425	85 - 6046
AP1	FOS:JUN	860	0.09	0	50412.92	24217	7302 - 60018

Co-location and overlapping DNA motifs of CTCF with another DNA motifs.

FR orientation of CTCF

Motif 1	Motif 2	No.	Mean of distances bet. DNA sites (nt)	Median of distances bet. DNA sites (nt)	Mean of distances from TSS (nt)	Median of distances from TSS (nt)	Interquartile range of distance from TSS (nt)
CTCF	SMC3	2876	0.01	0	34606.92	13716	3073 - 39471
CTCF	RAD21	2352	0.00	0	33492.68	12913	2824 - 37672
CTCF	CTCFL	1151	0.00	0	30252.04	11606	2229 - 34539
CTCF	ZBTB7A	470	0.27	0	23227.96	7065	745 - 23496
CTCF	E2F	123	0.81	0	7913.36	222	61 - 1997
CTCF	WT1	120	0.00	0	3543.72	114	44 - 375
CTCF	MYC	110	2.30	0	31289.45	11948	2887 - 33972

RF orientation of CTCF

Motif 1	Motif 2	No.	Mean of distances bet. DNA sites (nt)	Median of distances bet. DNA sites (nt)	Mean of distances from TSS (nt)	Median of distances from TSS (nt)	Interquartile range of distance from TSS (nt)
CTCF	RXRA	1362	0.00	0	29981.33	10937	2100 - 31407
CTCF	CTCFL	429	0.00	0	25171.22	9834	1859 - 24741
CTCF	RAD21	337	0.00	0	38829.91	17973	6117 - 45749
CTCF	ZIC1	126	1.40	0	35480.65	10286	2316 - 29380
CTCF	ZIC3	108	0.00	0	30219.32	10904	4463 - 31037

767

768 **References**

769

770 Ackerman SL, Minden AG, Williams GT, Bobonis C, Yeung CY. 1991. Functional
771 significance of an overlapping consensus binding motif for Sp1 and Zif268 in
772 the murine adenosine deaminase gene promoter. *Proc Natl Acad Sci U S A* **88**:
773 7523-7527.
774 Ansari AZ, Peterson-Kaufman KJ. 2011. A partner evokes latent differences between
775 Hox proteins. *Cell* **147**: 1220-1221.
776 Bailey SD, Zhang X, Desai K, Aid M, Corradin O, Cowper-Sal Lari R, Akhtar-Zaidi B,
777 Scacheri PC, Haibe-Kains B, Lupien M. 2015. ZNF143 provides sequence
778 specificity to secure chromatin interactions at gene promoters. *Nat Commun* **2**:
779 6186.
780 Barutcu AR, Lajoie BR, Fritz AJ, McCord RP, Nickerson JA, van Wijnen AJ, Lian JB,
781 Stein JL, Dekker J, Stein GS et al. 2016. SMARCA4 regulates gene expression
782 and higher-order chromatin structure in proliferating mammary epithelial cells.
783 *Genome research* **26**: 1188-1201.
784 Chatterjee R, Zhao J, He X, Shlyakhtenko A, Mann I, Waterfall JJ, Meltzer P,
785 Sathyanarayana BK, FitzGerald PC, Vinson C. 2012. Overlapping ETS and CRE
786 Motifs ((G/C)CGGAAGTGACGTCA) preferentially bound by GABPalpha and
787 CREB proteins. *G3 (Bethesda)* **2**: 1243-1256.
788 Chen M, Manley JL. 2009. Mechanisms of alternative splicing regulation: insights from
789 molecular and genomics approaches. *Nat Rev Mol Cell Biol* **10**: 741-754.
790 Das D, Clark TA, Schweitzer A, Yamamoto M, Marr H, Arribere J, Minovitsky S,
791 Poliakov A, Dubchak I, Blume JE et al. 2007. A correlation with exon
792 expression approach to identify cis-regulatory elements for tissue-specific
793 alternative splicing. *Nucleic acids research* **35**: 4845-4857.
794 de Wit E, Vos ES, Holwerda SJ, Valdes-Quezada C, Verstegen MJ, Teunissen H,
795 Splinter E, Wijchers PJ, Krijger PH, de Laat W. 2015. CTCF Binding Polarity
796 Determines Chromatin Looping. *Molecular cell* **60**: 676-684.
797 Guo Y, Xu Q, Canzio D, Shou J, Li J, Gorkin DU, Jung I, Wu H, Zhai Y, Tang Y et al.
798 2015. CRISPR Inversion of CTCF Sites Alters Genome Topology and

799 Enhancer/Promoter Function. *Cell* **162**: 900-910.
800 He X, Syed KS, Tillo D, Mann I, Weirauch MT, Vinson C. 2015. GABPalpha Binding
801 to Overlapping ETS and CRE DNA Motifs Is Enhanced by CREB1: Custom
802 DNA Microarrays. *G3 (Bethesda)* **5**: 1909-1918.
803 Hsu SC, Gilgenast TG, Bartman CR, Edwards CR, Stonestrom AJ, Huang P, Emerson
804 DJ, Evans P, Werner MT, Keller CA et al. 2017. The BET Protein BRD2
805 Cooperates with CTCF to Enforce Transcriptional and Architectural Boundaries.
806 *Molecular cell* **66**: 102-116 e107.
807 Jolma A, Yan J, Whitington T, Toivonen J, Nitta KR, Rastas P, Morgunova E, Enge M,
808 Taipale M, Wei G et al. 2013. DNA-binding specificities of human transcription
809 factors. *Cell* **152**: 327-339.
810 Jolma A, Yin Y, Nitta KR, Dave K, Popov A, Taipale M, Enge M, Kivioja T, Morgunova
811 E, Taipale J. 2015. DNA-dependent formation of transcription factor pairs alters
812 their binding specificity. *Nature* **527**: 384-388.
813 Jung I, Schmitt A, Diao Y, Lee AJ, Liu T, Yang D, Tan C, Eom J, Chan M, Chee S et al.
814 2019. A compendium of promoter-centered long-range chromatin interactions in
815 the human genome. *Nature genetics* **51**: 1442-1449.
816 Karolchik D, Barber GP, Casper J, Clawson H, Cline MS, Diekhans M, Dreszer TR,
817 Fujita PA, Guruvadoo L, Haeussler M et al. 2014. The UCSC Genome Browser
818 database: 2014 update. *Nucleic acids research* **42**: D764-770.
819 Katainen R, Dave K, Pitkanen E, Palin K, Kivioja T, Valimaki N, Gylfe AE, Ristolainen
820 H, Hanninen UA, Cajuso T et al. 2015. CTCF/cohesin-binding sites are
821 frequently mutated in cancer. *Nature genetics* **47**: 818-821.
822 Kel AE, Gossling E, Reuter I, Cheremushkin E, Kel-Margoulis OV, Wingender E. 2003.
823 MATCH: A tool for searching transcription factor binding sites in DNA
824 sequences. *Nucleic acids research* **31**: 3576-3579.
825 Kheradpour P, Kellis M. 2014. Systematic discovery and characterization of regulatory
826 motifs in ENCODE TF binding experiments. *Nucleic acids research* **42**:
827 2976-2987.
828 Kin K, Chen X, Gonzalez-Garay M, Fakhouri WD. 2016. The effect of non-coding
829 DNA variations on P53 and cMYC competitive inhibition at cis-overlapping
830 motifs. *Hum Mol Genet* **25**: 1517-1527.
831 Kulakovskiy IV, Vorontsov IE, Yevshin IS, Sharipov RN, Fedorova AD, Rumynskiy EI,

832 Medvedeva YA, Magana-Mora A, Bajic VB, Papatsenko DA et al. 2018.
833 HOCOMOCO: towards a complete collection of transcription factor binding
834 models for human and mouse via large-scale ChIP-Seq analysis. *Nucleic acids*
835 *research* **46**: D252-D259.
836 Li H, Durbin R. 2009. Fast and accurate short read alignment with Burrows-Wheeler
837 transform. *Bioinformatics (Oxford, England)* **25**: 1754-1760.
838 Lieberman-Aiden E, van Berkum NL, Williams L, Imakaev M, Ragoczy T, Telling A,
839 Amit I, Lajoie BR, Sabo PJ, Dorschner MO et al. 2009. Comprehensive
840 mapping of long-range interactions reveals folding principles of the human
841 genome. *Science (New York, NY)* **326**: 289-293.
842 McLean CY, Bristor D, Hiller M, Clarke SL, Schaar BT, Lowe CB, Wenger AM,
843 Bejerano G. 2010. GREAT improves functional interpretation of cis-regulatory
844 regions. *Nature biotechnology* **28**: 495-501.
845 Merabet S, Mann RS. 2016. To Be Specific or Not: The Critical Relationship Between
846 Hox And TALE Proteins. *Trends Genet* **32**: 334-347.
847 Mumbach MR, Satpathy AT, Boyle EA, Dai C, Gowen BG, Cho SW, Nguyen ML,
848 Rubin AJ, Granja JM, Kazane KR et al. 2017. Enhancer connectome in primary
849 human cells identifies target genes of disease-associated DNA elements. *Nature*
850 *genetics* **49**: 1602-1612.
851 Neph S, Kuehn MS, Reynolds AP, Haugen E, Thurman RE, Johnson AK, Rynes E,
852 Maurano MT, Vierstra J, Thomas S et al. 2012. BEDOPS: high-performance
853 genomic feature operations. *Bioinformatics (Oxford, England)* **28**: 1919-1920.
854 Newburger DE, Bulyk ML. 2009. UniPROBE: an online database of protein binding
855 microarray data on protein-DNA interactions. *Nucleic acids research* **37**:
856 D77-82.
857 Osato N. 2018. Characteristics of functional enrichment and gene expression level of
858 human putative transcriptional target genes. *BMC Genomics* **19**: 957.
859 Portales-Casamar E, Thongjuea S, Kwon AT, Arenillas D, Zhao X, Valen E, Yusuf D,
860 Lenhard B, Wasserman WW, Sandelin A. 2010. JASPAR 2010: the greatly
861 expanded open-access database of transcription factor binding profiles. *Nucleic*
862 *acids research* **38**: D105-110.
863 Purmann A, Toedling J, Schueler M, Carninci P, Lehrach H, Hayashizaki Y, Huber W,
864 Sperling S. 2007. Genomic organization of transcriptomes in mammals:

865 Coregulation and cofunctionality. *Genomics* **89**: 580-587.
866 Rao SS, Huntley MH, Durand NC, Stamenova EK, Bochkov ID, Robinson JT, Sanborn
867 AL, Machol I, Omer AD, Lander ES et al. 2014. A 3D map of the human
868 genome at kilobase resolution reveals principles of chromatin looping. *Cell* **159**:
869 1665-1680.
870 Schreiber J, Libbrecht M, Bilmes J, Noble W. 2017. Nucleotide sequence and DNaseI
871 sensitivity are predictive of 3D chromatin architecture. *bioRxiv*.
872 Sherwood RI, Hashimoto T, O'Donnell CW, Lewis S, Barkal AA, van Hoff JP, Karun V,
873 Jaakkola T, Gifford DK. 2014. Discovery of directional and nondirectional
874 pioneer transcription factors by modeling DNase profile magnitude and shape.
875 *Nature biotechnology* **32**: 171-178.
876 Shlyueva D, Stampfel G, Stark A. 2014. Transcriptional enhancers: from properties to
877 genome-wide predictions. *Nature reviews Genetics* **15**: 272-286.
878 Shrivastava A, Calame K. 1994. An analysis of genes regulated by the multi-functional
879 transcriptional regulator Yin Yang-1. *Nucleic acids research* **22**: 5151-5155.
880 Slattery M, Riley T, Liu P, Abe N, Gomez-Alcala P, Dror I, Zhou T, Rohs R, Honig B,
881 Bussemaker HJ et al. 2011. Cofactor binding evokes latent differences in DNA
882 binding specificity between Hox proteins. *Cell* **147**: 1270-1282.
883 Tabuchi TM, Deplancke B, Osato N, Zhu LJ, Barrasa MI, Harrison MM, Horvitz HR,
884 Walhout AJ, Hagstrom KA. 2011. Chromosome-biased binding and gene
885 regulation by the Caenorhabditis elegans DRM complex. *PLoS Genet* **7**:
886 e1002074.
887 van Helden J. 2003. Regulatory sequence analysis tools. *Nucleic acids research* **31**:
888 3593-3596.
889 Wang ET, Sandberg R, Luo S, Khrebtukova I, Zhang L, Mayr C, Kingsmore SF,
890 Schroth GP, Burge CB. 2008. Alternative isoform regulation in human tissue
891 transcriptomes. *Nature* **456**: 470-476.
892 Wang J, Vicente-Garcia C, Seruggia D, Molto E, Fernandez-Minan A, Neto A, Lee E,
893 Gomez-Skarmeta JL, Montoliu L, Lunyak VV et al. 2015. MIR retrotransposon
894 sequences provide insulators to the human genome. *Proc Natl Acad Sci U S A*
895 **112**: E4428-4437.
896 Wang J, Zhuang J, Iyer S, Lin X, Whitfield TW, Greven MC, Pierce BG, Dong X,
897 Kundaje A, Cheng Y et al. 2012a. Sequence features and chromatin structure

898 around the genomic regions bound by 119 human transcription factors. *Genome*
899 *research* **22**: 1798-1812.
900 Wang L, Wang S, Li W. 2012b. RSeQC: quality control of RNA-seq experiments.
901 *Bioinformatics (Oxford, England)* **28**: 2184-2185.
902 Wei Z, Gao F, Kim S, Yang H, Lyu J, An W, Wang K, Lu W. 2013. Klf4 organizes
903 long-range chromosomal interactions with the oct4 locus in reprogramming and
904 pluripotency. *Cell Stem Cell* **13**: 36-47.
905 Weintraub AS, Li CH, Zamudio AV, Sigova AA, Hannett NM, Day DS, Abraham BJ,
906 Cohen MA, Nabet B, Buckley DL et al. 2017. YY1 Is a Structural Regulator of
907 Enhancer-Promoter Loops. *Cell* **171**: 1573-1588 e1528.
908 Wingender E, Dietze P, Karas H, Knuppel R. 1996. TRANSFAC: a database on
909 transcription factors and their DNA binding sites. *Nucleic acids research* **24**:
910 238-241.
911 Xi H, Yu Y, Fu Y, Foley J, Halees A, Weng Z. 2007. Analysis of overrepresented motifs
912 in human core promoters reveals dual regulatory roles of YY1. *Genome research*
913 **17**: 798-806.
914 Xie X, Lu J, Kulbokas EJ, Golub TR, Mootha V, Lindblad-Toh K, Lander ES, Kellis M.
915 2005. Systematic discovery of regulatory motifs in human promoters and 3'
916 UTRs by comparison of several mammals. *Nature* **434**: 338-345.
917 Xie X, Mikkelsen TS, Gnirke A, Lindblad-Toh K, Kellis M, Lander ES. 2007.
918 Systematic discovery of regulatory motifs in conserved regions of the human
919 genome, including thousands of CTCF insulator sites. *Proc Natl Acad Sci U S A*
920 **104**: 7145-7150.
921 Xie Z, Hu S, Blackshaw S, Zhu H, Qian J. 2010. hPDI: a database of experimental
922 human protein-DNA interactions. *Bioinformatics (Oxford, England)* **26**:
923 287-289.
924 Yardimci GG, Ozadam H, Sauria MEG, Ursu O, Yan KK, Yang T, Chakraborty A, Kaul
925 A, Lajoie BR, Song F et al. 2019. Measuring the reproducibility and quality of
926 Hi-C data. *Genome Biol* **20**: 57.
927 Yoon SO, Chikaraishi DM. 1992. Tissue-specific transcription of the rat tyrosine
928 hydroxylase gene requires synergy between an AP-1 motif and an overlapping E
929 box-containing dyad. *Neuron* **9**: 55-67.
930 Zhang H, Li F, Jia Y, Xu B, Zhang Y, Li X, Zhang Z. 2017. Characteristic arrangement

931 of nucleosomes is predictive of chromatin interactions at kilobase resolution.
932 *Nucleic acids research* **45**: 12739-12751.
933 Zhang Y, Liu T, Meyer CA, Eeckhoute J, Johnson DS, Bernstein BE, Nusbaum C,
934 Myers RM, Brown M, Li W et al. 2008. Model-based analysis of ChIP-Seq
935 (MACS). *Genome Biol* **9**: R137.
936 Zhao Y, Stormo GD. 2011. Quantitative analysis demonstrates most transcription factors
937 require only simple models of specificity. *Nature biotechnology* **29**: 480-483.
938